© 2015. Published by The Company of Biologists Ltd | Journal of Cell Science (2015) 128, 645–655 doi:10.1242/jcs.132720

RESEARCH ARTICLE

Retromer and the dynamin Vps1 cooperate in the retrieval of transmembrane proteins from vacuoles

Henning Arlt[1], Fulvio Reggiori[2] and Christian Ungermann[1,*]

ABSTRACT

Endosomes are dynamic organelles that need to combine the ability to successfully deliver proteins and lipids to the lysosome-like vacuole, and recycle others to the Golgi or the plasma membrane. We now show that retromer, which is implicated in retrieval of proteins from endosomes to the Golgi or to the plasma membrane, can act on vacuoles. We explore its function using an assay that allows us to dissect the required cofactors during recycling. We demonstrate that recycling of the transmembrane receptor Vps10 from vacuoles requires the retromer, the dynamin-like Vps1, and the Rab7 GTPase Ypt7. Retromer and Vps1 leave the vacuole together with the cargo, whereas Ypt7 stays behind, in agreement with its regulatory function. Recycled cargo then accumulates at endosomes and later at the Golgi, implying consecutive sorting steps to the final destination. Our data further suggest that retromer and Vps1 are essential to maintain vacuole membrane organization. Taken together, our data demonstrate that retromer can cooperate with Vps1 and the Rab Ypt7 to clear the vacuole of selected membrane proteins.

KEY WORDS: Retromer, Vps1, Dynamin, Vacuole, Recycling, Endosomal trafficking

INTRODUCTION

Vesicular transport within eukaryotic cells depends on a conserved protein machinery to sort cargo into forming vesicles, transport them to the next organelle and mediate the final fusion of the vesicle with the target membrane. A common principle of these transport processes is the recycling of the sorting machinery to make it available for further rounds of transport. In the case of peripheral membrane proteins, such as coat or tethering proteins, recycling occurs simply through their release from the carriers. For membrane proteins that are involved in vesicular transport, more sophisticated processes are necessary to ensure their availability because recycling has to be coordinated with the retrograde transport of membranes from the target organelle. Based on a mathematical model, Heinrich and Rapoport have proposed that low-affinity interactions during sorting should be sufficient to generate transport gradients that rely on recycling and reuse of respective fusion and fission machinery (Heinrich and Rapoport, 2005). Several examples have been described that support this idea. For instance, the endosomal SNARE Vti1 interacts with epsinR (Miller et al., 2007), and sortilin and the cation-independent mannose-6-phosphate receptor depend on the retromer complex for their recycling (Harbour et al., 2010; Harterink et al., 2011; Seaman, 2004; Seaman et al., 2009).

Several transport pathways deliver lipids and proteins to the vacuole, including the endocytic and biosynthetic pathways, the adaptor protein (AP)-3 pathway, the constitutive selective type of autophagy called the cytosol–vacuole-transport pathway, and general autophagy (Bowers and Stevens, 2005). To maintain the size and functionality of vacuoles, however, excess lipids and sorting proteins need to be recycled. There are indications that vacuoles employ microautophagy as a means to counterbalance the surface growth (Müller et al., 2000; Sattler and Mayer, 2000), although this process seems to be mainly active during starvation. Some studies have suggested that there is active recycling from the vacuole (Bryant et al., 1998; Dove et al., 2004). In metazoan cells, the process of autophagic lysosomal reformation (ALR) includes a fission process to recycle membrane proteins and membranes for the reformation of lysosomes after fusion with the autophagosome (Chen et al., 2014). The process includes the formation of vesicular lysosomal structures, which depends on the AP-2 adaptor, clathrin and dynamin 2 (Rong et al., 2012; Schulze et al., 2013). However, whether a similar machinery is also required on vacuoles is not known.

On endosomes, the retromer has been characterized as a major protein complex involved in recycling of membrane proteins to the Golgi and plasma membrane (Bonifacino and Hurley, 2008; Seaman, 2012; Seaman et al., 1998; Seaman et al., 1997). Substrates of the retromer include, in metazoan cells, the mannose-6-phosphate receptor and the Wnt transporter Wntless, and, in yeast, Vps10 (Harterink et al., 2011; Seaman et al., 1997). Vps10 is a single-pass type-I transmembrane protein with a large luminal N-terminus that binds cargo molecules and a small cytosolic C-terminus that contains sorting signals for retrieval (Cooper and Stevens, 1996). The retromer contains two subcomplexes. The dimeric sorting nexin (SNX) complex consists of Vps5 (in metazoans SNX1 or SNX2) and Vps17 (in metazoans SNX5, SNX6 or SNX32), which possess N-BAR domains to deform membranes (van Weering et al., 2012b) and the phosphatidylinositol-3-phosphate-binding PX domain (Burda et al., 2002). The second subcomplex is formed by the trimeric cargo-recognition complex (CRC) composed of Vps26, Vps29 and Vps35 (Hierro et al., 2007; Seaman et al., 1998). The central subunit of the CRC is Vps35, which binds to the late endosomal Rab GTPase Rab7 or, in yeast, to Ypt7 (Balderhaar et al., 2010; Liu et al., 2012; Nakada-Tsukui et al., 2005; Rojas et al., 2008; Seaman et al., 2009). In addition, mammalian retromer can interact with the Rab7 GTPase-activating

[1]University of Osnabrück, Department of Biology/Chemistry, Biochemistry section, Barbarastrasse 13, 49076 Osnabrück, Germany. [2]University Medical Centre Utrecht, Department of Cell Biology, Center for Molecular Medicine, Heidelberglaan 100, 3584 CX Utrecht, The Netherlands.

*Author for correspondence (cu@uos.de)

Received 20 June 2014; Accepted 9 December 2014

Journal of Cell Science (2015) 128, 645–655 doi:10.1242/jcs.132720

protein (GAP) TBC1D5 (Seaman et al., 2009). Based on structural analyses and *in vitro* remodeling assays, it has been postulated that retromer sorts membrane proteins into a tubular structure, which eventually fuses with the Golgi (Hierro et al., 2007; van Weering et al., 2012b; van Weering et al., 2012a). However, how retromer deforms the membrane, sorts cargo and releases tubules, remains elusive and most models have remained untested due to the lack of appropriate assays.

Here, we have developed an assay to follow membrane protein recycling from the vacuole. Exploiting this new assay, we have been able to reveal that the retromer can recycle Vps10 from vacuoles in a similar manner to endosomal recycling. This event also requires active Ypt7 and the dynamin homolog Vps1. Our data thus demonstrate that the retromer is a versatile membrane protein recycling complex that has activity beyond the endosome.

RESULTS

A recycling assay for vacuole-localized transmembrane proteins

The retromer is known to act on endosomal membranes to recycle protein-sorting receptors back to the Golgi. However, Vps35, a subunit of the retromer CRC, has also been detected on the vacuolar membrane (Liu et al., 2012) (Fig. 1A). Recruitment of Vps35 to the vacuole depends on active Ypt7, whereas endosomal localization requires the sorting nexin (SNX) subunits Vps5 and Vps17 (Liu et al., 2012). This prompted us to also analyze the localization of Vps26 and Vps29, the other two CRC subunits and interestingly we could also detect their partial overlap with the vacuolar marker FM4-64 (Fig. 1A), suggesting that the entire CRC can associate to vacuoles. We also detected some Vps17, a subunit of the retromer SNX complex on vacuoles; however, much weaker than CRC subunits (Fig. 1A). A known retromer

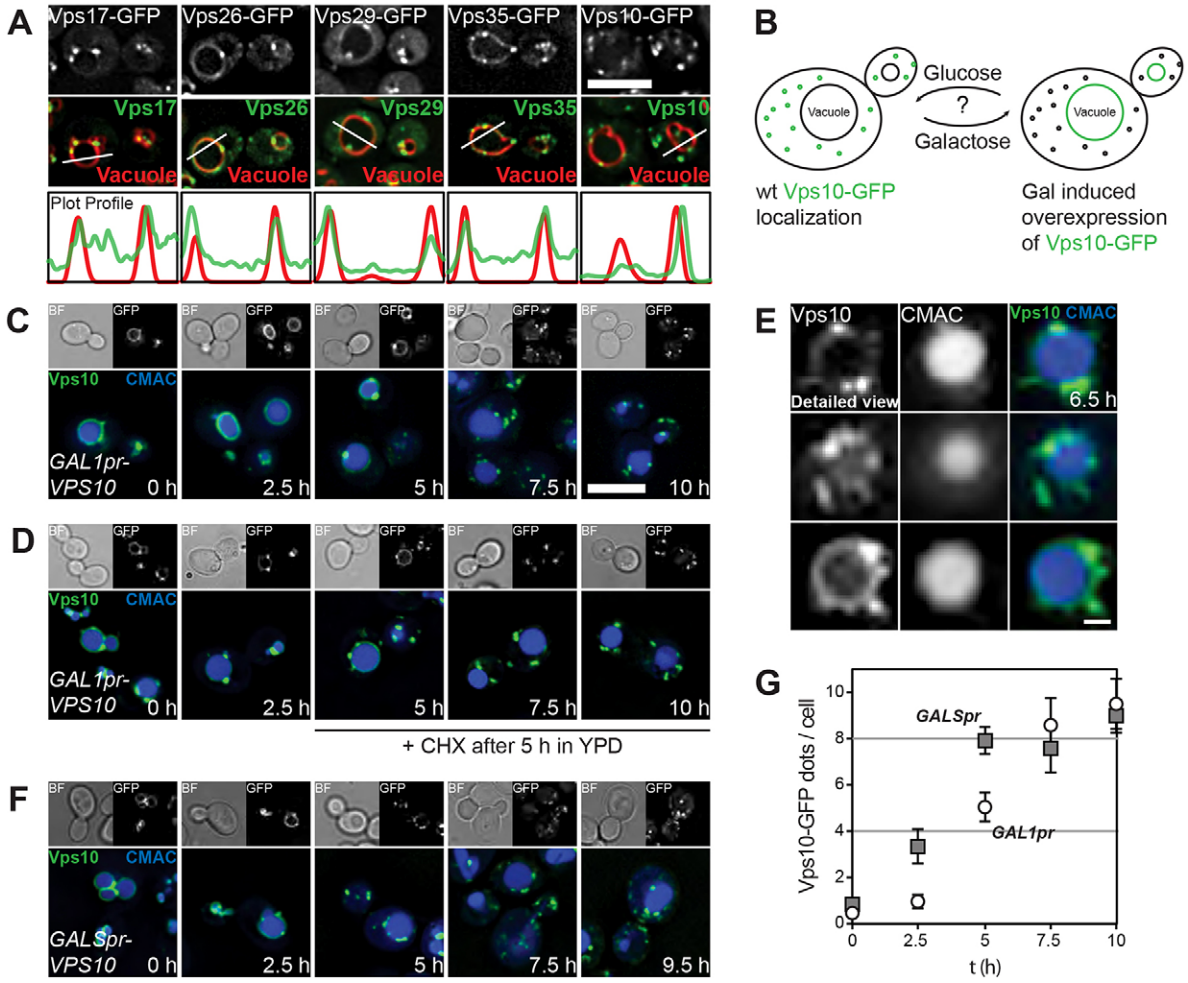

Fig. 1. Vps10–GFP can be recycled from vacuoles. (A) Localization of endogenous GFP-tagged retromer subunits. Vacuole membrane was visualized by FM4-64 staining as described in the Materials and Methods. Fluorescence intensity plots of representative vacuoles are shown (indicated by white lines). Scale bar: 5 μm. (B) Model of Vps10 trafficking from endosomes and Golgi to the vacuole under overexpression conditions and the putative removal mechanism from the vacuole. (C) Recycling of Vps10–GFP from vacuoles. Expression of Vps10–GFP under the control of the *GAL1* promoter was stopped by shifting cells from YPG to YPD medium as described in the Materials and Methods. Time points refer to time in YPD after the medium replacement. Scale bar: 5 μm. (D) Vps10 relocalization is not due to new protein synthesis. Cycloheximide was added 5 h after transfer into YPD and images were taken as in C. (E) Detailed views of Vps10 localization after 6.5 h in YPD. The experiment was carried out as in C. Scale bar: 1 μm. (F) Recycling kinetics from vacuoles correlate with Vps10 load on vacuoles. Vps10–GFP was expressed from the weaker *GALS* promoter and the distribution of this chimera was analyzed as in C. (G) Quantification of assays shown in C and D. Results are mean±s.d. of Vps10–GFP dots/cell as determined on sum projections of 3.2-μm stacks taken at the respective time point. Between 67 and 127 cells were counted in each frame.

Journal of Cell Science (2015) 128, 645–655 doi:10.1242/jcs.132720

cargo is the transmembrane protein Vps10, the sorting receptor for various vacuolar hydrolases including carboxypeptidase Y, which shares some structural similarities with the metazoan mannose-6-phosphate receptor (Marcusson et al., 1994). In contrast to retromer, Vps10 was exclusively found to display a punctate localization, which very likely correspond to endosomes and the Golgi (Fig. 1A), as shown previously (Chi et al., 2014). Thus, it was unclear which function retromer performed on the vacuole. We thus hypothesized that retromer is required to recycle transmembrane proteins from the vacuolar membrane.

To address this question, we decided to analyze whether retromer is able to recycle Vps10 from the vacuolar limiting membrane. It has been shown that Vps10 is largely displaced to the vacuolar membrane upon overexpression (Cereghino et al., 1995) or in mutants that inhibit its recycling from the endosome (Burda et al., 2002). We took advantage of this phenotype to study the recycling of the vacuolar Vps10 pool. We expected that this surplus of Vps10 would have two consequences. First, we thought that an increase of cargo would allow us to more easily monitor retromer function by live-cell imaging on vacuoles, which can easily be distinguished morphologically from the much smaller endosomes. Second, we expected a strong delay in the retrieval, as the pool of Vps10 was much larger than the available machinery.

For our assay, we overexpressed Vps10–GFP from the inducible *GAL1* promoter. Once Vps10 was completely localized to the vacuole, cells were shifted from galactose-containing medium to glucose-containing medium to repress further expression. Subsequently, the localization of Vps10 was analyzed at different time points after the shift to the glucose-containing medium (Fig. 1B). Indeed, when we expressed a pulse of functional *VPS10-GFP* from its chromosomal locus under control of the strong *GAL1* promoter, Vps10 was completely shifted to the vacuolar membrane and only few fluorescent puncta were visible (Fig. 1C). After the shift to glucose medium, Vps10 initially remained on vacuoles and then started to accumulate in dots on the vacuolar membrane after 5 h. After 7.5 h, most Vps10 localized in dot-like structures (Fig. 1C,G), with a distribution profile similar to endogenous Vps10 (Fig. 1A). Importantly, the appearance of Vps10 puncta was not due to newly expressed protein, because the addition of cycloheximide, a potent translation inhibitor added after 5 h, did not block the relocalization into dots (Fig. 1D). When we took a closer look at cells during this relocalization of Vps10, we observed Vps10-positive tubular structures emanating from the vacuole (Fig. 1E). Thus, the dot-like appearance of Vps10 is a likely consequence of its recycling from the vacuolar membrane.

We noticed that the shift of Vps10 from a vacuolar to the dot-like localization required a relatively long time compared to other intracellular transport processes. We reasoned that this might be due to the high amount of cargo on the vacuole, which likely sequesters the recycling machinery. We therefore predicted that lowering of the overexpression would result in faster recycling of Vps10. This was indeed the case. When *VPS10* was expressed from the weaker *GALS* promoter, the shift from vacuole to puncta was observed by 2.5 h (Fig. 1F, see Fig. 1G for quantification).

Recycling from vacuoles depends on the retromer, Ypt7 and Vps1

To identify the machinery involved in the recycling process, we deleted selected genes and analyzed the efficiency of Vps10 recycling using our assay. In the absence of any retromer subunit, recycling from the vacuole was blocked (Fig. 2A,C), indicating that Vps10 is also recognized on vacuoles. To our surprise, Vps10 was not localized to dots on the vacuolar membrane after 5–7.5 h in this strain, which indicates that retromer might need to concentrate cargo before removal from the vacuole. This phenotype became even more evident when the intensity of the Vps10–GFP signal on vacuoles was compared between wild-type and *vps26Δ* cells (Fig. 2B). Deletion of the vacuolar Rab protein Ypt7 or inactivation by deletion of the guanine-nucleotide-exchange factor (GEF) subunit Mon1 also blocked recycling (Fig. 2C, see below). The process is independent of the machinery needed for vacuole inheritance, because *vac8* and *vac7* mutants allowed efficient recycling from the vacuole. This demonstrates that the dilution of vacuolar Vps10 during cell division and vacuole inheritance do not explain the delay in Vps10 recycling from vacuoles. Recycling was also independent of the batten-disease proteins Btn1, Btn2 and Btn3, which are involved in endosome–Golgi trafficking and bind to Vps26 (Kama et al., 2011; Kama et al., 2007), or mutants of the AP-3 pathway (Fig. 2C). Interestingly, absence of the yeast dynamin Vps1, which has recently been implicated in endosomal recycling mediated by retromer (Chi et al., 2014), strongly impaired recycling (Fig. 2C, see below). However, a deletion of *Mvp1*, a protein that interacts with Vps1 (Ekena and Stevens, 1995) and is involved in endosomal recycling (Chi et al., 2014), was without effect (Fig. 2C,D). Furthermore, an *mvp1* deletion did not lead to mislocalization of Vps10 to the vacuole, when expressed from its normal promoter. This is in contrast to retromer mutants, like *vps26Δ*, that show vacuolar localization of Vps10 under these conditions (Fig. 2H). This suggests that the requirements for recycling from the vacuole differ from those on endosomes, where Mvp1 is part of the general recycling machinery (Chi et al., 2014).

To understand the spatiotemporal order of the proteins involved in recycling, we analyzed the localization of retromer on vacuoles relative to its cargo during the Vps10 recycling process. To achieve this, we traced GFP-tagged Vps10 together with functional RFP-tagged retromer subunits over time. The retromer subunit Vps17, which is involved in tubule formation on endosomes (van Weering et al., 2012b), readily localized to Vps10-positive dots on the vacuolar membrane (Fig. 2E). This dot-like localization persisted over time as Vps10 left the vacuole surface. The CRC subunit Vps35 also colocalized strongly with Vps10-positive structures on the vacuole, on Vps10-positive tubules and, finally, on the Vps10 dots after release from the vacuole (Fig. 2F). To further address whether retromer was specifically recycling Vps10 from the vacuole, we truncated parts of the cytosolic C-terminus of Vps10 where two putative retrieval signals reside (Cooper and Stevens, 1996), resulting in the Vps10ΔC construct. Recycling of overexpressed Vps10ΔC from the vacuole was blocked efficiently (Fig. 2G) and endogenously expressed Vps10ΔC from the *VPS10* promoter resulted in mislocalization to the vacuole comparable to Vps10 localization in retromer mutants (Fig. 2H). Our data thus agree with a role of the entire retromer in recycling Vps10 from the vacuole surface.

The removal of Vps10 from the vacuole was relatively slow, probably because overexpression of the cargo sequesters the recycling machinery (see above). We thus wondered whether retromer would also be able to recycle cargo from the vacuole more rapidly under a more native condition without employing overexpression. To test this, we made use of a haploid yeast strain

Journal of Cell Science (2015) 128, 645–655 doi:10.1242/jcs.132720

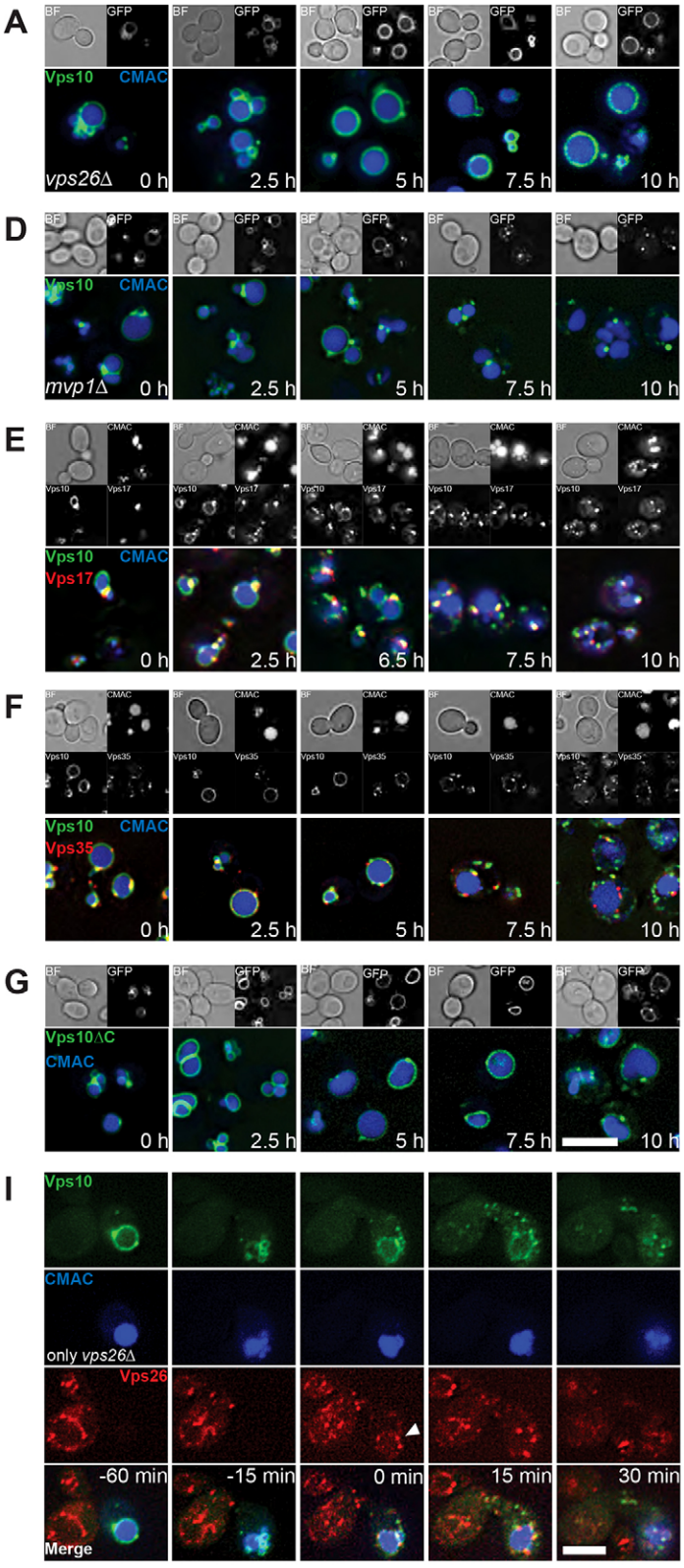

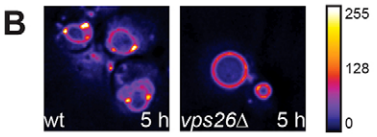

C

Function / Complex	Mutant	Vps10 recycling
Retromer	*vps26Δ*	defective
	vps5Δ	defective
	vps29Δ	defective
	vps35Δ	defective
Endosomal Rab/GEF	*ypt7Δ*	defective
	mon1Δ	defective
Rab GAPs	*msb3Δ*	normal
	msb4Δ	normal
	gyp7Δ	normal
Vacuole Inheritance	*vac8Δ*	normal
	vac7Δ	normal
AP-3 sorting	*apl5Δ*	normal
Endosome to Golgi trafficking	*btn1Δ*	normal
	btn2Δ	normal
	btn3Δ	normal
Golgi trafficking	*erv14Δ*	normal
Dynamin	*vps1Δ*	defective
Sorting Nexins	*mvp1Δ*	normal

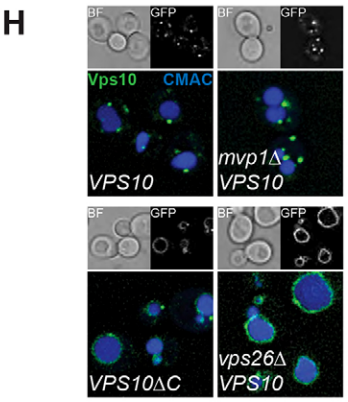

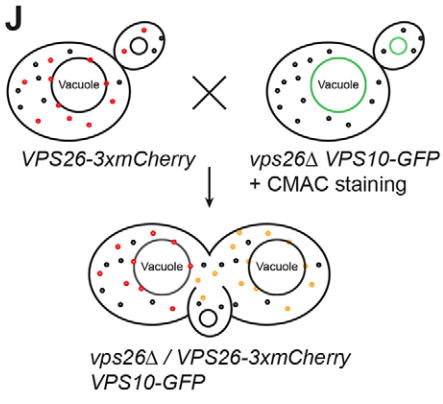

Fig. 2. See next page for legend.

carrying a retromer deletion, which results in mislocalization of endogenously expressed Vps10–GFP to the vacuole, as previously shown (Cereghino et al., 1995; Markgraf et al., 2009). To complement the retromer mutant, we mixed this strain with another haploid wild-type strain of opposing mating type, which expressed functional Vps26 tagged with 3×mCherry. We then monitored mating of these strains in a microfluidics chamber over time (Fig. 2I,J). After incubation of both strains for

Journal of Cell Science

Journal of Cell Science (2015) 128, 645–655 doi:10.1242/jcs.132720

Fig. 2. Vps10 recycling from vacuoles depends on the retromer, Ypt7 and Vps1. Vps10–GFP recycling from vacuoles was investigated as in Fig. 1. (A,B,D–G) Vps10–GFP was overexpressed under the control of the *GAL1* promoter before shifting cells to YPD as described in Fig. 1. (A) Deletion of *VPS26* blocks accumulation and release of Vps10 from vacuoles. (B) Vps10–GFP is concentrated on vacuoles during release. Wild-type and *vps26Δ* cells were investigated as in Fig. 1. The 5-h time-point after the shift to glucose medium is shown. The signal intensity of the Vps10–GFP signal is displayed using the 'fire' lookup table (see right bar). (C) Overview of the results obtained with the different analyzed deletion mutants. Vps10–GFP was expressed in all deletion mutants from the *GAL1* promoter and analyzed as in A. (D) Deletion of *MVP1* has no effect on recycling of Vps10 from the vacuole. (E,F) Retromer subunits localize to Vps10 dots on the vacuole during retrograde transport from this organelle. Endogenous retromer subunits Vps17 and Vps35 were C-terminally tagged with mCherry. (G) Recycling of C-terminally truncated Vps10–GFP is blocked. The C-terminal 89 amino acids of Vps10 were removed by introduction of the GFP tag at this site, resulting in Vps10ΔC. The construct was expressed from the *GAL1* promoter in its chromosomal locus and recycling of the chimera was assayed as in A. (H) Wild-type *VPS10-GFP* and *VPS10ΔC-GFP* were expressed from their chromosomal locus under control of the *VPS10* promoter, and localization of the proteins was analyzed as in Fig. 1A. Localization of Vps10 was also analyzed in the *vps26Δ* and *mvp1Δ* mutants. (I,J) Mating assay of a strain expressing *VPS10-GFP* in a *vps26Δ* background with a wild-type strain expressing *VPS26-3xmCherry*. Only the *vps26Δ* was stained with CMAC to monitor vacuole morphology. See scheme in J and details in Materials and Methods. Time points indicate time after or before mating. The white arrowhead indicates the first appearance of mCherry signal in the diploid cell directly after mating. Scale bars: 5 µm.

~90 min, cells started to mate. Immediately after mating, Vps26–3×mCherry localized to the Vps10–GFP-positive vacuole (Fig. 2I, white arrow), which resulted in release of most Vps10 from the vacuole into dot-like structures within 15–30 min after mating (Fig. 2I). This experiment demonstrates that the retromer can rapidly recycle Vps10 from the vacuole.

Vps1 supports fission of retromer-positive tubules on vacuoles

Vps1 is involved in retromer function at endosomes (Chi et al., 2014), and is required for the recycling of Vps10 from vacuoles, as shown here (Fig. 2C). To understand the role of Vps1 in more detail, we followed Vps10–GFP in the *vps1* mutant over time, and realized that it strongly accumulated on vacuoles in dot-like structures (Fig. 3A) and not along the rim as in retromer mutants (Fig. 2A). These structures persisted over time and finally resulted in tubular extensions that protruded away from the vacuole surface (Fig. 3A). On these tubules, Vps10–GFP sometimes accumulated on the tips (see detailed view, yellow arrow). These data are consistent with a scission role of Vps1 in recycling Vps10 from the vacuole and agree with the previously observed vacuolar localization of Vps1 (Peters et al., 2004).

To follow Vps1 during this process, we tagged Vps1 with a C-terminal mCherry tag. This tagged version is only partially active on vacuoles as Vps10–GFP did not completely relocalize into dots after the time course, but it did allow us to follow Vps1 relative to the Vps10 cargo. When we analyzed the localization of Vps1–mCherry during vacuolar recycling of Vps10, some Vps1 puncta on the vacuole could be detected after 7.5 and 10 h, which were also positive for Vps10. These data suggest that the Vps1 fission activity might be involved in the formation of Vps10-positive structures. Given that Vps10–GFP was still concentrated into dots and tubules on the vacuolar membrane in the *vps1Δ* mutant, we wondered where retromer would localize during the time course. Like in the wild-type situation, CRC and SNX subunits of the retromer localized after 5 h to the vacuolar dot-like Vps10 accumulations (Fig. 3C,D). However, retromer stayed on the dot-like structures even at later time points, and was sometimes colocalized with Vps10–GFP on the tubular structures emanating from the vacuole (Fig. 3C,D, detailed view).

We then analyzed the retrieval of Vps10 from the vacuole at the ultrastructural level by electron microscopy. In comparison to the wild-type, *vps1Δ* cells displayed various phenotypes at both 7.5 and 10 h after transfer to glucose medium, including accumulation of endosomal structures, remnants of vacuole homotypic fusion events and more inwards budding profiles at the vacuole limiting membrane. Moreover, electron-dense protrusions emerging from the vacuole surface, which very likely represent the Vps10-positive tubules, were exclusively observed in the *vps1Δ* mutant. These profiles were more abundant at 10 h than at 7.5 h in agreement with the light microscopy results (Fig. 3A,E–H).

To analyze a possible role of Vps1 in retromer function more directly, we deleted *vps1* in cells expressing chomosomally GFP-tagged retromer subunits without overexpression of Vps10. In the wild-type, Vps35 as well as Vps26 localized to endosomes, vacuolar membranes and the cytoplasm, whereas Vps17 was only localized to puncta and the cytoplasm (Fig. 1A; Fig. 3I). In the *vps1Δ* mutant, however, the subcellular localization of the retromer shifted entirely to dot-like structures, and both the vacuolar membrane staining and the cytoplasmic background were lost. In combination, our data indicate that Vps1 is necessary to separate retromer-positive tubules from vacuoles and eventually allow for the release of the retromer subunits into the cytosol during both endosomal and vacuolar recycling.

Vacuolar Vps10 recycles to the endosome and then to the Golgi

To understand the fate of the Vps10 cargo during recycling from vacuoles, we analyzed to which organelle the Vps10-positive structures would be directed. As Vps10 resides on endosomes and the Golgi in wild-type cells, we used Ypt6 and Sec7 as Golgi marker proteins and Vps8 as an endosomal marker protein for our experimental setup. Vps8 colocalized with ~30% of Vps10 right from the beginning. This suggests that either some of the vacuolar Vps8 corresponds to perivacuolar late endosomes or that the excess Vps10 cargo drives some Vps8 to the vacuole. This colocalization increased dramatically from 30% to 70% during the first 5 h of the assay, when Vps10 starts accumulating in puncta away from the vacuole. Interestingly, colocalization of Vps8 with Vps10 decreased after 5 h until a level of ~60% was reached (Fig. 4A,C). In comparison, the Golgi marker Ypt6 showed nearly no colocalization with Vps10 within the first 5 h of the assay. After this time point, however, colocalization increased up to 20% (Fig. 4B,C). Similar observations were made when we analyzed Sec7–mCherry localization relative to that of Vps10–GFP. Intriguingly, the gradual loss of colocalization with Vps8 after 5 h of the recycling assay was compensated for by colocalization with the Golgi markers (Fig. 4C). We therefore suggest that the recycling pathway from the vacuole mediated by the retromer is initially directed towards endosomes and subsequently from endosomes to the Golgi.

Crosstalk of Ypt7 with the retromer during recycling

The retromer interacts with both metazoan Rab7 and yeast Ypt7, although the precise role of Ypt7/Rab7 has not been clarified. As cells lacking Ypt7 had a defect in Vps10 recycling from vacuoles

Journal of Cell Science (2015) 128, 645–655 doi:10.1242/jcs.132720

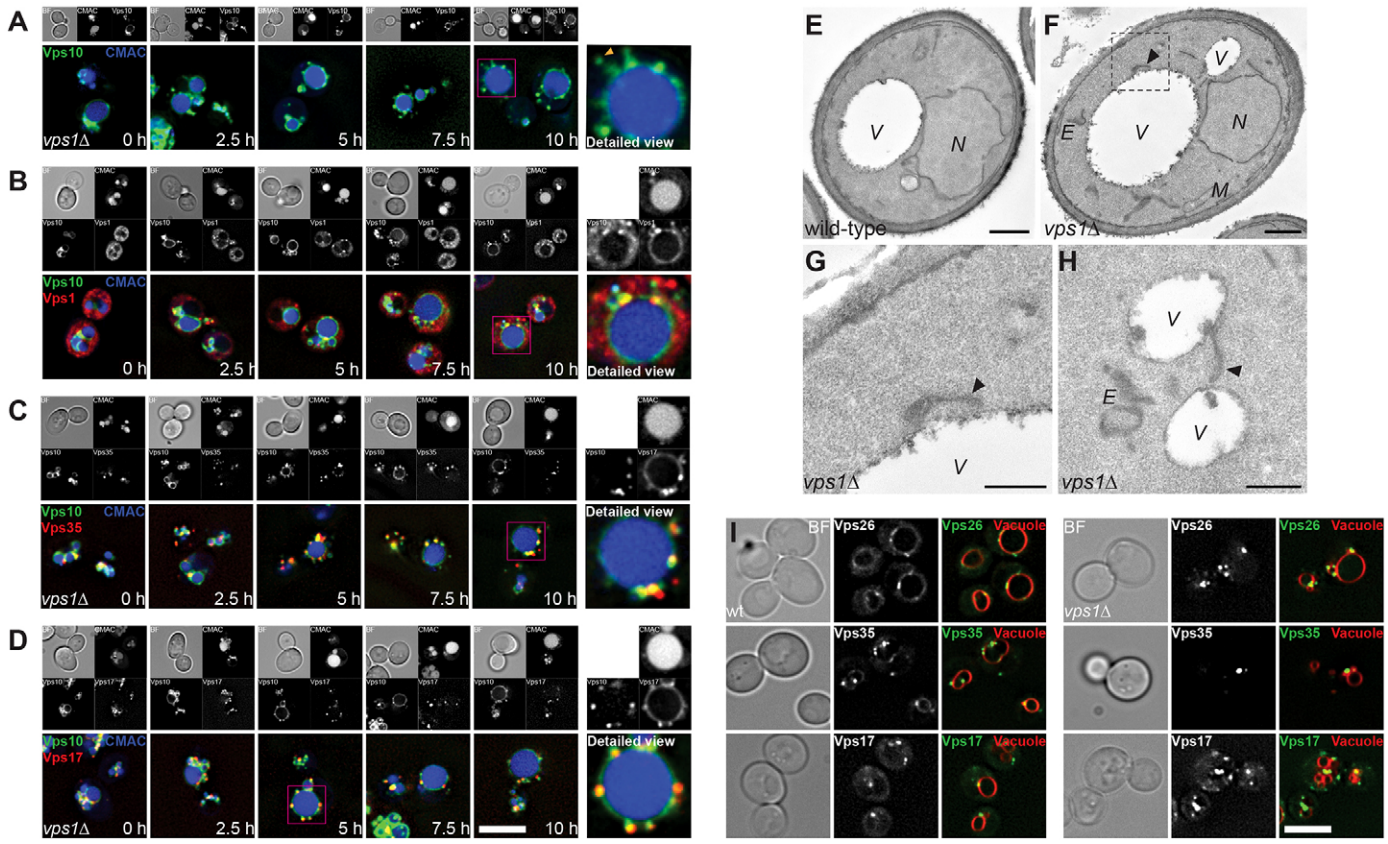

Fig. 3. Vps1 is involved in Vps10 recycling from vacuoles. (A,C,D) Retrieval of Vps10–GFP in *vps1Δ* cells after overexpression from the *GAL1* promoter. Analysis was performed as in Fig. 1C. (A) Deletion of *VPS1* results in a block of Vps10 recycling from vacuoles. (B) Vps1 colocalizes with Vps10 concentration profiles during vacuolar recycling. Vps1 was C-terminally tagged with mCherry in the *GAL1pr-VPS10-GFP* test strain. The assay was carried out as in A. The yellow arrowhead indicates tubular structures enriched in Vps10–GFP. Note that C-terminal tagging partially affects Vps1 function. (C,D) Vps35–mCherry (C) and Vps17–mCherry (D) localize to the sites where Vps10 concentrates in the *vps1Δ* mutant. Red boxes indicate areas shown at higher magnification. Scale bar: 5 µm. (E–H) Ultrastructural analysis in wild-type (E) and *vps1Δ* strains (F–H). Cells were treated as in Fig. 1C before being processed for electron microscopy as indicated in the Materials and Methods. E and F show entire cells, while panels G (region indicated by the dashed box in panel F) and H highlight the tubules (arrowheads) emerging from the vacuole observed in the *vps1Δ* mutant, which are seen as electron-dense protrusions. E, endosome; M, mitochondrion; N, nucleus; V, vacuole. Scale bars: 500 nm (E,F), 200 nm (G,H). (I) Deletion of *vps1* leads to accumulation of retromer on endosomes. Retromer subunits were C-terminally tagged with GFP and expressed from their chromosomal locus. Vacuoles were stained with FM4-64 as described in Materials and Methods. Scale bars: 5 µm (A–D,I).

(Fig. 2C), we decided to try and clarify the role of the GTPase in more detail. We initially revisited observations on the localization of endogenously expressed Vps10–GFP. Vps10–GFP is found in multiple puncta in wild-type cells, whereas loss of retromer function in the *vps26Δ* mutant results in total relocalization of Vps10–GFP to the vacuole, as detected by FM4-64 staining (Fig. 5A,B). Interestingly, endogenously expressed Vps10–GFP remains in dots in *ypt7*Δ cells, even though these cells have small and clearly visible vacuoles. Similar observations on Vps10 localization were made with cells lacking the Ypt7 GEF subunit Mon1 (Liu et al., 2012). When we quantified the amount of vacuole-localized Vps10 by colocalization with the vacuolar dye FM4-64, we observed a similarly low colocalization in the *ypt7Δ* mutant as in wild-type cells (Fig. 5B). Only in the double mutant (*vps26*Δ *ypt7*Δ) did Vps10 again colocalize with FM4-64 as in the *vps26*Δ mutant. The consequences of a loss of Ypt7 are thus clearly different from a retromer mutant, indicating that the retromer might still perform some of its functions on endosomes even if Ypt7 is absent.

We then turned to our system where excess cargo is present on vacuoles. When we analyzed *ypt7*Δ or *mon1*Δ cells, we observed a clear block of Vps10–GFP release from the vacuole surface (Fig. 5C,D). We then tagged Ypt7 with mCherry to analyze its behavior relative to the Vps10 cargo. At early time points, Ypt7 strongly colocalized to sites of Vps10-positive structures (Fig. 5E). However, Ypt7 remained on vacuoles during and after the release of Vps10 (Fig. 5E, 7.5 h time point), suggesting that Ypt7 is involved in the activation of the recycling process but is not part of the machinery itself. When we followed the dynamics of Vps10 during release after 7 h, we could observe Vps10 in mobile dots on the vacuolar membrane (Fig. 5F, yellow arrowheads). However, Ypt7 did not accumulate in these structures. Our combined data indicate that Ypt7 stays on the donor membrane and is not part of the tubular structure.

The retromer and Vps1 affect vacuole homeostasis

Having demonstrated that retromer also functions on vacuoles using our assay, we next asked whether retromer and Vps1 could be involved in vacuole membrane homeostasis. Vps1 has been previously linked to vacuole biogenesis and was shown to affect not only vacuole fission but also fusion (Alpadi et al., 2013; Peters et al., 2004). The *vps1Δ* mutant has a defect in *in vitro*

Journal of Cell Science (2015) 128, 645–655 doi:10.1242/jcs.132720

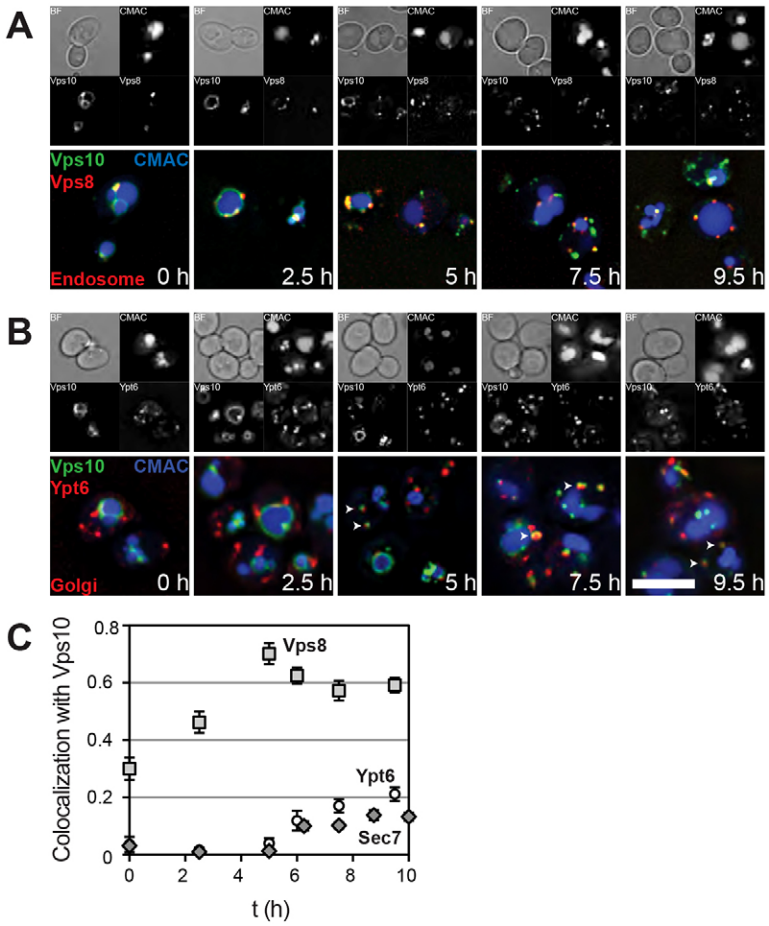

Fig. 4. Vacuolar retrieval of Vps10 is directed first to endosomes and then to the Golgi. Vps10–GFP recycling was followed as in Fig. 1C with *GAL1*-promoter-induced overexpression. Golgi and endosome marker proteins were tagged C-terminally with mCherry. (A) Vps10 colocalizes with the endosomal marker protein Vps8 during recycling from vacuoles. (B) N-terminal mCherry-tagged Ypt6 colocalizes with Vps10 at later time-points of the recycling process. White arrowheads highlight colocalizations. (C) Quantification of the colocalization of Vps10–GFP during retrograde transport with Golgi and endosome marker proteins (see Materials and Methods for details). Results are mean±s.e.m. (n=25–100 cells/time point). Scale bars: 5 µm.

vacuole fusion, and recombinant Vps1 interacts with the SNARE Vam3 (Peters et al., 2004). We reasoned that at least some of these observations would also be consistent with a retromer function in the recycling of SNARE proteins from the vacuole. Recycling and reuse of SNAREs after fusion is, for example, well described in the fusion of synaptic vesicles with the plasma membrane (Jahn and Fasshauer, 2012), but such a pathway has not been described for vacuoles or lysosomes to date.

As deletions of retromer and Vps1 affect the localization of Vps10–GFP on vacuoles in our recycling assay (Fig. 2A; Fig. 3A), we wondered whether the steady-state localization of vacuolar SNAREs might change in these mutants. Curiously, we observed that Vam3 changed from showing a smooth and equal distribution along wild-type vacuoles (Fig. 6A) to a dot-like localization in the *vps35*Δ mutant (Fig. 6B). Likewise, GFP-tagged Vam3 was similarly concentrated in *vps1*Δ cells (Fig. 6C). This redistribution was not due to a general redistribution of vacuolar proteins, given that the vacuolar (V)-ATPase subunit Vma2 was not localized to Vam3-positive dots (Fig. 6D). Moreover, this effect was not due to a change in Vam3 levels in *vps35*Δ cells (Fig. 6E). Other SNAREs like Vti1, Nyv1 or Pep12 did not change their localization pattern upon retromer deletion (supplementary material Fig. S1). We thus postulate that retromer and Vps1 affect the membrane homeostasis of vacuoles.

Because retromer and Vps1 affect the distribution of Vam3 similarly, we wondered whether this would have an effect on Vam3 functionality in vacuolar fusion, as previously observed for the *vps1*Δ mutant (Kulkarni et al., 2014; Peters et al., 2004). Fusion can be measured *in vitro* using isolated vacuoles from two tester strains. One strain is deleted for a vacuolar peptidase (BJ3505 *pep4Δ*) and the other strain lacks alkaline phosphatase (DKY *pho8Δ*). Upon fusion of vacuoles from these strains, the peptidase cleaves the inactive phosphatase. The amount of fusion can then be measured by assaying the activity of active phosphatase (Haas et al., 1994). When we analyzed fusion of vacuoles from *vps1Δ* or retromer mutants, we could detect a block of fusion in the *vps1Δ* as described previously (Kulkarni et al., 2014; Peters et al., 2004) and a similar defect for the retromer mutants (Fig. 6F). Importantly, this defect in fusion was not due to mislocalization of the marker proteins Pho8 or Pep4 to the vacuole, because addition of recombinant Vam7 SNARE protein, which can promote SNARE- and HOPS-driven fusion on vacuoles (Thorngren et al., 2004), was able to rescue fusion of all mutants (Fig. 6F). This observation is consistent with the idea that a fraction of SNAREs are trapped in a complex with retromer or Vps1 upon deletion of the other recycling factor. The addition of Vam7 then either liberates Vam3 or uses the available SNAREs to rescue fusion. These data provide support that retromer and Vps1 have a crucial role in controlling vacuole membrane homeostasis.

DISCUSSION

Our data provide detailed mechanistic insights into retromer function. Our assay, which exploits an excess of its natural substrate, the Vps10 cargo receptor, has allowed us to dissect the machinery involved in membrane recycling from the vacuole and

Journal of Cell Science (2015) 128, 645–655 doi:10.1242/jcs.132720

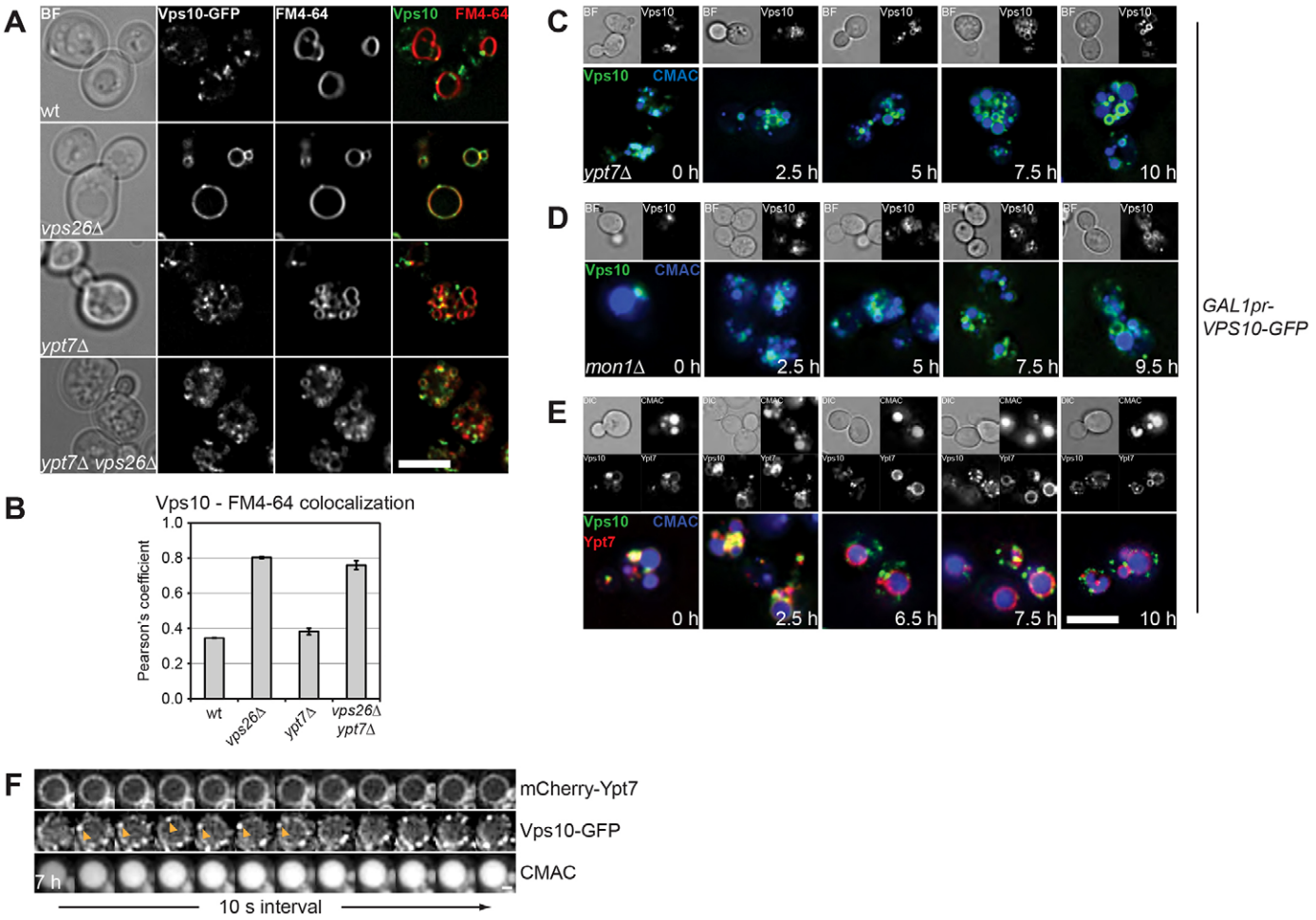

Fig. 5. Ypt7 is essential for retromer-mediated retrograde transport from the vacuole. (A) Localization of Vps10–GFP in wild-type, and *vps26Δ*, *ypt7Δ* and *vps26Δ ypt7Δ* mutant strains. Vacuoles were stained with FM4-64. (B) Quantification of Vps10 colocalization with the vacuolar membrane marker FM4-64. Quantification of total fluorescence correlation in A was carried out using the JacoP software. Results are mean±s.e.m. (n=45–133). (C,D) Active Ypt7 is required for Vps10–GFP recycling. Deletion of Ypt7 (C) or the GEF Mon1 (D) leads to a block in Vps10–GFP retrieval. Analysis was performed as in Fig. 1c using *GAL1*-promoter-mediated overexpression of *VPS10*. (E) Localization of Ypt7 during the recycling process. N-terminal mCherry-tagged Ypt7 distribution was compared to that of Vps10-GFP over time. Assay was carried out as in D. (F) Dynamics of Vps10-positive structures relative to Ypt7 on vacuoles. A time course analysis of cells in shown in E was performed 7 h after transfer into YPD. Single-plane images of GFP, mCherry and DAPI channels were acquired every 10 s for a period of 2 min. Yellow arrows indicate Vps10–GFP-positive structures moving on the vacuolar membrane. Scale bars: 5 µm (A,E); 1 µm (F).

the order of events with an unprecedented detail (see Fig. 6G for a model). We demonstrate here that the retromer concentrates cargo prior to its release through a tubule (Fig. 1; Fig. 2B). Once a tubule is formed, Vps1 mediates the fission of this tubule (Fig. 3) and retromer release into the cytoplasm occurs probably only after this fission event (Fig. 3). We also provide strong evidence that the Rab GTPase Ypt7 is initially required for retromer function at the membrane but does not enter the tubule (Fig. 5). This demonstrates that retromer can recycle proteins from the vacuolar membrane. Finally, our data provide evidence that vacuoles from retromer and Vps1 mutants behave similarly, i.e. they both have a homotypic fusion defect, which could be reversed by the addition of a soluble Vam7 SNARE. This fusion defect agrees with the misorganization of SNAREs in *vps35Δ* and *vps1Δ* mutants on vacuole membranes, indicating that Vps1 and retromer are involved in the homeostasis of this organelle.

A previous study on the endosomal function of retromer provided evidence that both Vps1 and the SNX-BAR protein Mvp1 cooperate in endosomal tubule formation (Chi et al., 2014). Our data nicely agree with a fission function of Vps1 on both endosomes and vacuoles, as Vps10-decorated tubules did not separate from vacuoles in *vps1*Δ cells. Moreover, Vps1 is not only needed for tubulation, but also to recycle retromer components. In the absence of Vps1, the retromer strongly accumulated on membranes (Fig. 3). This accumulation will limit the available pool of this complex, which as a limiting factor will block further retrograde transport events. In contrast to the findings on endosomal membranes, we did not find evidence for a role of Mvp1 in retromer-mediated recycling from vacuoles, suggesting that the two processes also differ in their requirements (Fig. 2). Vps1 has previously been implicated in endocytosis (Nannapaneni et al., 2010; Smaczynska-de Rooij et al., 2012), similar to the known role of dynamin (Cocucci et al., 2012). At present, we do not yet know how Vps1 is recruited to the retromer tubules.

How is retromer function coordinated on membranes? As all retromer subunits behaved similar in our assays, and all retromer mutants resulted in the same recycling defect, we suspect that the

Journal of Cell Science (2015) 128, 645–655 doi:10.1242/jcs.132720

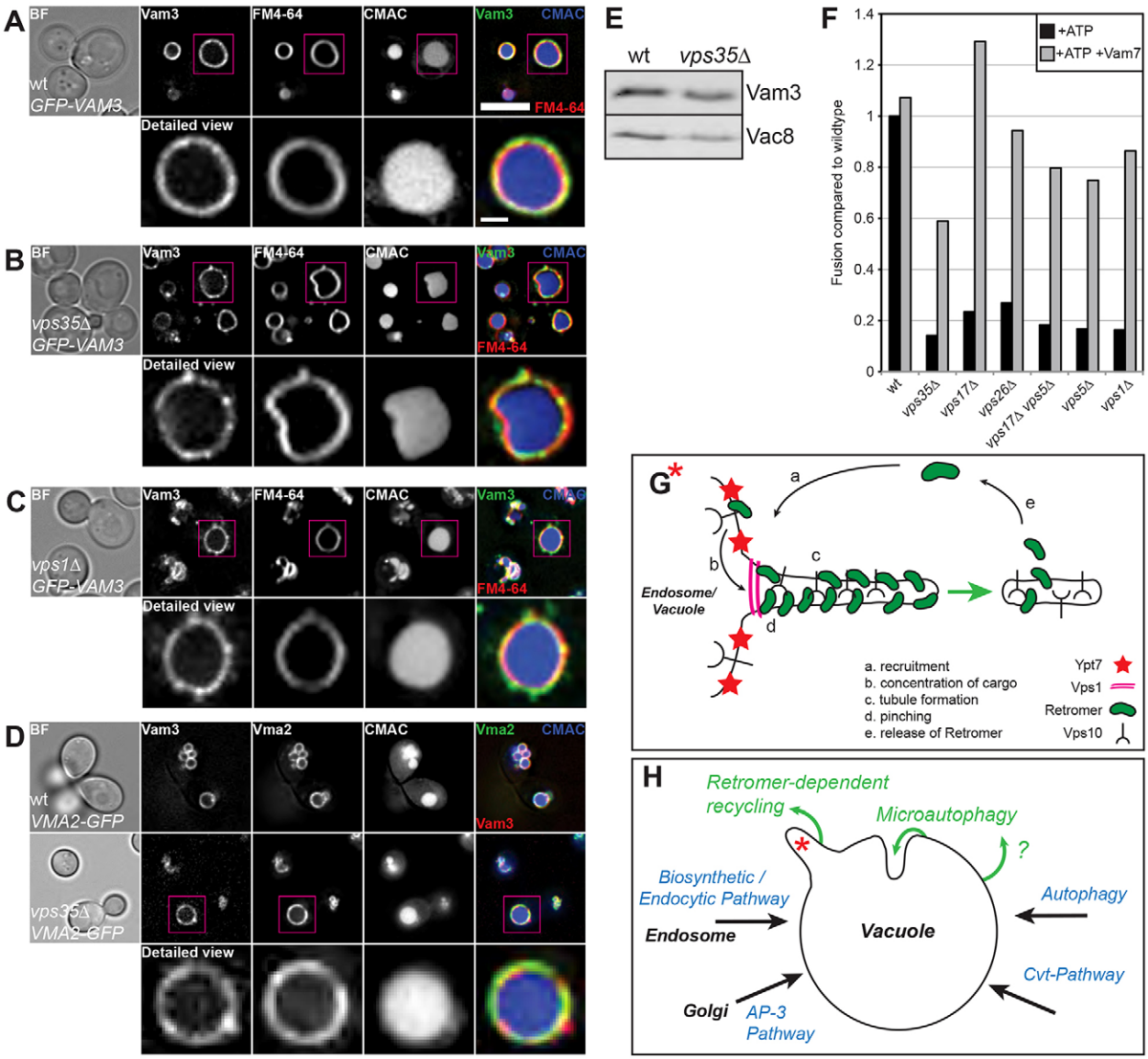

Fig. 6. Retromer and Vps1 are involved in vacuole homeostasis. (A–C) Loss of the retromer or Vps1 results in an altered localization of Vam3. Chromosomal GFP–Vam3 was expressed from the *PHO5* promoter. Localization was analyzed in wild-type (A), *vps35Δ* (B) and *vps1Δ* (C) cells. The vacuole lumen and membrane were stained with CMAC and FM4-64, respectively, as described in the Materials and Methods. Scale bars: 5 µm, normal view; 1 µm, detailed view. (D) Endogenous Vma2 was C-terminally tagged with GFP. RFP–Vam3 was expressed from a centromeric plasmid. (E) Comparison of Vam3 levels in wild-type and *vps35Δ*. Vacuoles from BJ wild-type (wt) and *vps35Δ* strains were isolated for the vacuole fusion assay as described in the Materials and Methods. An equal amount of vacuoles was separated by SDS-PAGE and analyzed by western blotting using antibodies against Vam3 and Vac8 as loading control. (F) Representative results of fusion assays with vacuoles isolated from retromer and *vps1* mutants. Deletions were generated in the *pep4Δ* background strain (BJ3505). Isolated BJ vacuoles were added to vacuoles from the DKY strain resuspended in the ATP-containing fusion buffer incubated for 90 min at 27˚C (black bars). Where indicated, 2 µM Vam7 was added to the fusion reaction (gray bars). A representative result is shown. Experiments were repeated at least two times. (G) Model for retromer function on endosomal and vacuolar membranes. (H) Model for trafficking of transmembrane proteins to and from the vacuole.

complex functions as one unit during the recycling process. This would agree with the initial identification of retromer (Seaman et al., 1998) and the fact that we could purify this complex as a heteropentamer (H.A., C.U., unpublished), even though the complex seems to separate into the two subcomplexes in metazoan cells (Hierro et al., 2007). Previous work has suggested that Ypt7 can coordinate retromer function on endosomes (Balderhaar et al., 2010; Liu et al., 2012), in agreement with work in mammalian cells (Rojas et al., 2008; Seaman et al., 2009). Inactivation of Ypt7 has been shown to cause accumulation of Vps10 on retromer-positive endosomes (Liu et al., 2012). However, endosomal recycling is not blocked completely, because Vps10 localizes to the vacuole in such a situation (Fig. 5). This suggests that Ypt7 is involved in organizing the coordination between recycling and endosome-vacuole fusion, although the exact mechanism is not yet clear. On vacuoles, we could demonstrate that Ypt7 is essential for Vps10 recycling, but is not part of the carrier released from the vacuole, whereas the retromer stays on Vps10-positive membranes (Fig. 5). Our data agree with a model in which the endosomal Ypt7–GTP that was activated by the Mon1–Ccz1 GEF, first engages in initiating recycling before HOPS-driven fusion occurs.

Any remaining Rab7/Ypt7 on endosomal tubules will then likely become substrate to a specific GAP that has been identified in complex with the retromer (Seaman et al., 2009). We tested whether GAP inactivation of Ypt7 is necessary for recycling, but deletion of the putative Ypt7 GAPs was without an effect on recycling efficiency (Fig. 2C). How Rab activity and turnover is coordinated during retromer-driven recycling needs further investigation.

Our analysis of retromer and Vps1 pools on vacuoles sheds light onto the general organization of membrane homeostasis at the vacuole. We observed here that the SNARE Vam3 is affected in its lateral organization in both mutants, whereas other vacuolar transmembrane proteins like the V-ATPase subunit Vma2 are not. SNAREs like Vti1 that also function on endosomes are likely substrates for a directed recycling process to provide sufficient machinery for further transport to the vacuole (Bryant et al., 1998; Dove et al., 2004). Although we could not detect a difference in localization of SNAREs other than Vam3, a defect in recycling must not necessarily be evident by a change in localization. However, we do not believe that the response of Vam3 is a special case here, but rather reflects a general change in the vacuole membrane homeostasis due to loss of retromer or Vps1. If Vps1 and retromer always cooperate at the vacuole, one expectation is that their deletion leads to similar consequences. Indeed, the defects in both membrane organization and fusion were similar in the *vps1Δ* and *vps35Δ* backgrounds, and fusion could be rescued by the same mechanism, i.e. the addition of the soluble SNARE Vam7 (Fig. 6F) (Thorngren et al., 2004). Whether the observed requirement of Vps1 for membrane fusion (Alpadi et al., 2013; Kulkarni et al., 2014; Peters et al., 2004) relates to either a fusion-specific function or rather to a consequence of a defect in recycling, needs further investigation. Our data show that the fusion defect applies to both retromer and *vps1* mutants, even though the fusion machinery is apparently present on vacuoles. Furthermore, some retromer mutants have fragmented vacuoles, indicating that retromer is involved in maintaining vacuoles that are competent for fusion.

We speculate that the Vps10-mediated membrane retrieval could also be part of a mechanism for quality control of vacuoles. The removal of transmembrane proteins from the vacuole is likely necessary to maintain vacuolar function and to change its composition in response to environmental changes. It could be also part of a process to control and avoid extensive vacuolar membrane expansion. Downregulation could occur by either microautophagy, recycling through the endomembrane system and subsequent sorting into intraluminal vesicles or a yet unidentified mechanism (Fig. 6H). These mechanisms might not be mutually exclusive as suggested by electron-microcopy-based observations on microautophagy, which showed that microautophagic tubules were largely devoid of membrane proteins (Müller et al., 2000). It will be important in future to identify the cargoes of retromer-mediated retrograde transport pathway revealed by this work to fully understand its relevance in the physiology of the vacuole.

MATERIALS AND METHODS

Yeast genetic manipulation and molecular biology

Saccharomyces cerevisiae strains used in this study are listed in supplementary material Table S1. Genetic manipulations were carried out by homologous recombination of overlapping PCR fragments as described previously (Janke et al., 2004; Longtine et al., 1998).

Light microscopy and image analysis

Cells were grown to logarithmic phase in yeast extract peptone (YP) medium containing glucose (YPD), galactose (YPG) or synthetic medium supplemented with essential amino acids (SDC). The vacuole membrane was stained with 30 µM FM4-64 for 30 min, followed by washing and incubation in medium without dye for 1 h before analysis (Vida and Emr, 1995). For luminal staining of vacuoles, cells were incubated in 0.1 mM 7-amino-4-chloromethylcoumarin (CMAC) for 10 min and washed with SDC medium.

To analyze the release of overexpressed Vps10–GFP from the vacuolar membrane, cells were grown in 10–20 ml YP medium containing 2% galactose for 18–22 h to logarithmic phase, washed and diluted in YP medium with 2% glucose, and analyzed by light microscopy after different times. Before collecting images, cells were always washed with synthetic medium containing glucose or galactose. To block protein synthesis, cycloheximide was added to a final concentration of 10 µg/ml.

Images were acquired on an Olympus IX-71 inverted microscope equipped with a 100× NA 1.49 objective, an sCMOS camera (PCO), an InsightSSI illumination system and SoftWoRx software (Applied Precision) or on a similar microscope equipped with a 100× NA 1.4 objective and CoolSNAP HQ2 camera (Photometrix, Tucson, AZ). *z*-stacks of 1–4 µm with 300-nm spacing were used for constrained-iterative deconvolution (SoftwoRx). Images were further processed using ImageJ. One representative plane of a *z*-stack is shown unless otherwise noted. Analysis of colocalization was either carried out using JACoP (Bolte and Cordelières, 2006) to determine Pearson's correlation coefficient of total fluorescence signals between two channels. Alternatively, an object-based approach was used, where single-point sources above a certain threshold are detected and overlap is quantified using a in-house ImageJ Plugin (H.A., Rainer Kurre, Jacob Piehler, C.U., unpublished).

Yeast mating assay

To analyze complementation of yeast mutants, haploid yeast cells carrying respective mutations in either MATa or α were grown to logarithmic phase as described above. One strain was stained with CMAC to distinguish different mating types, followed by thorough mixing of both strains. The mixture was applied to CellASIC Onix Y04C microfluidics chambers (Merck Millipore) and incubated under constant SDC medium exchange for 90 min at 23℃ prior to image acquisition.

Electron microscopy

Cells were processed for electron microscopy examination as previously described (Griffith et al., 2008).

Vacuole fusion

Vacuoles were isolated from BJ3505 or DKY2168 strains (see supplementary material Table S1) followed by mild lysis of spheroblasts and centifugation in a Ficoll step gradient as described (Haas, 1995). Fusion reactions were set up in 30 µl with 3 µg of each vacuole type (BJ and DKY), 125 mM KCl, 5 mM $MgCl_2$, 20 mM sorbitol, 1 mM Pipes-KOH pH 6.8 supplemented with 10 µM CoA, 10 ng His-Sec18 with or without an ATP regeneration system for 90 min at 26℃. 2 µM of recombinant His-Vam7 was added where indicated. Reactions were developed by addition of p-nitrophenyl phosphate to detergent-solubilized membranes to measure the absorbance at 400 nm of the alkaline-phosphatase-generated nitro-phenol. Background absorbance of samples lacking ATP was subtracted from original values.

Acknowledgements

We thank Markus Babst and the Ungermann laboratory for suggestions throughout this project, and Angela Perz and Despina Xanthakis for expert technical assistance.

Competing interests

The authors declare no competing or financial interests.

Author contributions

H.A. conducted all experiments except for EM experiments carried out by F.R. H.A. and C.U. designed experiments and wrote the manuscript.

Funding

This work was supported by the Deutsche Forschungsgemeinschaft (DFG); Sonderforschungbereich (SFB) 944 (project P11); and by the Hans-Mühlenhoff foundation (to C.U.). H.A. received support by a fellowship of the Deutsche Akademische Auslandsdienst (DAAD). F.R. is supported by ALW Open Program of the NWO (Netherlands Organisation for Scientific Research) [grant numbers 821.02.017 and 822.02.014]; a DFG-NWO cooperation [grant number DN82-303]; and The Netherlands Organisation for Health Research and Development (ZonMW) VICI [grant number 016.130.606].

Supplementary material

Supplementary material available online at
http://jcs.biologists.org/lookup/suppl/doi:10.1242/jcs.132720/-/DC1

References

Alpadi, K., Kulkarni, A., Namjoshi, S., Srinivasan, S., Sippel, K. H., Ayscough, K., Zieger, M., Schmidt, A., Mayer, A., Evangelista, M. et al. (2013). Dynamin-SNARE interactions control trans-SNARE formation in intracellular membrane fusion. *Nat. Commun.* **4**, 1704-1708.

Balderhaar, H. J. K., Arlt, H., Ostrowicz, C., Bröcker, C., Sündermann, F., Brandt, R., Babst, M. and Ungermann, C. (2010). The Rab GTPase Ypt7 is linked to retromer-mediated receptor recycling and fusion at the yeast late endosome. *J. Cell Sci.* **123**, 4085-4094.

Bolte, S. and Cordelières, F. P. (2006). A guided tour into subcellular colocalization analysis in light microscopy. *J. Microsc.* **224**, 213-232.

Bonifacino, J. S. and Hurley, J. H. (2008). Retromer. *Curr. Opin. Cell Biol.* **20**, 427-436.

Bowers, K. and Stevens, T. H. (2005). Protein transport from the late Golgi to the vacuole in the yeast Saccharomyces cerevisiae. *Biochim. Biophys. Acta* **1744**, 438-454.

Bryant, N. J., Piper, R. C., Weisman, L. S. and Stevens, T. H. (1998). Retrograde traffic out of the yeast vacuole to the TGN occurs via the prevacuolar/endosomal compartment. *J. Cell Biol.* **142**, 651-663.

Burda, P., Padilla, S. M., Sarkar, S. and Emr, S. D. (2002). Retromer function in endosome-to-Golgi retrograde transport is regulated by the yeast Vps34 PtdIns 3-kinase. *J. Cell Sci.* **115**, 3889-3900.

Cereghino, J. L., Marcusson, E. G. and Emr, S. D. (1995). The cytoplasmic tail domain of the vacuolar protein sorting receptor Vps10p and a subset of VPS gene products regulate receptor stability, function, and localization. *Mol. Biol. Cell* **6**, 1089-1102.

Chen, R., Zou, Y., Mao, D., Sun, D., Gao, G., Shi, J., Liu, X., Zhu, C., Yang, M., Ye, W. et al. (2014). The general amino acid control pathway regulates mTOR and autophagy during serum/glutamine starvation. *J. Cell Biol.* **206**, 173-182.

Chi, R. J., Liu, J., West, M., Wang, J., Odorizzi, G. and Burd, C. G. (2014). Fission of SNX-BAR-coated endosomal retrograde transport carriers is promoted by the dynamin-related protein Vps1. *J. Cell Biol.* **204**, 793-806.

Cocucci, E., Aguet, F., Boulant, S. and Kirchhausen, T. (2012). The first five seconds in the life of a clathrin-coated pit. *Cell* **150**, 495-507.

Cooper, A. A. and Stevens, T. H. (1996). Vps10p cycles between the late-Golgi and prevacuolar compartments in its function as the sorting receptor for multiple yeast vacuolar hydrolases. *J. Cell Biol.* **133**, 529-541.

Dove, S. K., Piper, R. C., McEwen, R. K., Yu, J. W., King, M. C., Hughes, D. C., Thuring, J., Holmes, A. B., Cooke, F. T., Michell, R. H. et al. (2004). Svp1p defines a family of phosphatidylinositol 3,5-bisphosphate effectors. *EMBO J.* **23**, 1922-1933.

Ekena, K. and Stevens, T. H. (1995). The Saccharomyces cerevisiae MVP1 gene interacts with VPS1 and is required for vacuolar protein sorting. *Mol. Cell. Biol.* **15**, 1671-1678.

Griffith, J., Mari, M., De Mazière, A. and Reggiori, F. (2008). A cryosectioning procedure for the ultrastructural analysis and the immunogold labelling of yeast Saccharomyces cerevisiae. *Traffic* **9**, 1060-1072.

Haas, A. (1995). A quantitative assay to measure homotypic vacuole fusion in vitro. *Methods Cell Sci.* **17**, 283-294.

Haas, A., Conradt, B. and Wickner, W. (1994). G-protein ligands inhibit in vitro reactions of vacuole inheritance. *J. Cell Biol.* **126**, 87-97.

Harbour, M. E., Breusegem, S. Y. A., Antrobus, R., Freeman, C., Reid, E. and Seaman, M. N. J. (2010). The cargo-selective retromer complex is a recruiting hub for protein complexes that regulate endosomal tubule dynamics. *J. Cell Sci.* **123**, 3703-3717.

Harterink, M., Port, F., Lorenowicz, M. J., McGough, I. J., Silhankova, M., Betist, M. C., van Weering, J. R. T., van Heesbeen, R. G. H. P., Middelkoop, T. C., Basler, K. et al. (2011). A SNX3-dependent retromer pathway mediates retrograde transport of the Wnt sorting receptor Wntless and is required for Wnt secretion. *Nat. Cell Biol.* **13**, 914-923.

Heinrich, R. and Rapoport, T. A. (2005). Generation of nonidentical compartments in vesicular transport systems. *J. Cell Biol.* **168**, 271-280.

Hierro, A., Rojas, A. L., Rojas, R., Murthy, N., Effantin, G., Kajava, A. V., Steven, A. C., Bonifacino, J. S. and Hurley, J. H. (2007). Functional architecture of the retromer cargo-recognition complex. *Nature* **449**, 1063-1067.

Jahn, R. and Fasshauer, D. (2012). Molecular machines governing exocytosis of synaptic vesicles. *Nature* **490**, 201-207.

Janke, C., Magiera, M. M., Rathfelder, N., Taxis, C., Reber, S., Maekawa, H., Moreno-Borchart, A., Doenges, G., Schwob, E., Schiebel, E. et al. (2004). A versatile toolbox for PCR-based tagging of yeast genes: new fluorescent proteins, more markers and promoter substitution cassettes. *Yeast* **21**, 947-962.

Kama, R., Robinson, M. and Gerst, J. E. (2007). Btn2, a Hook1 ortholog and potential Batten disease-related protein, mediates late endosome-Golgi protein sorting in yeast. *Mol. Cell. Biol.* **27**, 605-621.

Kama, R., Kanneganti, V., Ungermann, C. and Gerst, J. E. (2011). The yeast Batten disease orthologue Btn1 controls endosome-Golgi retrograde transport via SNARE assembly. *J. Cell Biol.* **195**, 203-215.

Kulkarni, A., Alpadi, K., Sirupangi, T. and Peters, C. (2014). A dynamin homolog promotes the transition from hemifusion to content mixing in intracellular membrane fusion. *Traffic* **15**, 558-571.

Liu, T.-T., Gomez, T. S., Sackey, B. K., Billadeau, D. D. and Burd, C. G. (2012). Rab GTPase regulation of retromer-mediated cargo export during endosome maturation. *Mol. Biol. Cell* **23**, 2505-2515.

Longtine, M. S., McKenzie, A., III, Demarini, D. J., Shah, N. G., Wach, A., Brachat, A., Philippsen, P. and Pringle, J. R. (1998). Additional modules for versatile and economical PCR-based gene deletion and modification in Saccharomyces cerevisiae. *Yeast* **14**, 953-961.

Marcusson, E. G., Horazdovsky, B. F., Cereghino, J. L., Gharakhanian, E. and Emr, S. D. (1994). The sorting receptor for yeast vacuolar carboxypeptidase Y is encoded by the VPS10 gene. *Cell* **77**, 579-586.

Markgraf, D. F., Ahnert, F., Arlt, H., Mari, M., Peplowska, K., Epp, N., Griffith, J., Reggiori, F. and Ungermann, C. (2009). The CORVET subunit Vps8 cooperates with the Rab5 homolog Vps21 to induce clustering of late endosomal compartments. *Mol. Biol. Cell* **20**, 5276-5289.

Miller, S. E., Collins, B. M., McCoy, A. J., Robinson, M. S. and Owen, D. J. (2007). A SNARE-adaptor interaction is a new mode of cargo recognition in clathrin-coated vesicles. *Nature* **450**, 570-574.

Müller, O., Sattler, T., Flötenmeyer, M., Schwarz, H., Plattner, H. and Mayer, A. (2000). Autophagic tubes: vacuolar invaginations involved in lateral membrane sorting and inverse vesicle budding. *J. Cell Biol.* **151**, 519-528.

Nakada-Tsukui, K., Saito-Nakano, Y., Ali, V. and Nozaki, T. (2005). A retromerlike complex is a novel Rab7 effector that is involved in the transport of the virulence factor cysteine protease in the enteric protozoan parasite Entamoeba histolytica. *Mol. Biol. Cell* **16**, 5294-5303.

Nannapaneni, S., Wang, D., Jain, S., Schroeder, B., Highfill, C., Reustle, L., Pittsley, D., Maysent, A., Moulder, S., McDowell, R. et al. (2010). The yeast dynamin-like protein Vps1:vps1 mutations perturb the internalization and the motility of endocytic vesicles and endosomes via disorganization of the actin cytoskeleton. *Eur. J. Cell Biol.* **89**, 499-508.

Peters, C., Baars, T. L., Bühler, S. and Mayer, A. (2004). Mutual control of membrane fission and fusion proteins. *Cell* **119**, 667-678.

Rojas, R., van Vlijmen, T., Mardones, G. A., Prabhu, Y., Rojas, A. L., Mohammed, S., Heck, A. J., Raposo, G., van der Sluijs, P. and Bonifacino, J. S. (2008). Regulation of retromer recruitment to endosomes by sequential action of Rab5 and Rab7. *J. Cell Biol.* **183**, 513-526.

Rong, Y., Liu, M., Ma, L., Du, W., Zhang, H., Tian, Y., Cao, Z., Li, Y., Ren, H., Zhang, C. et al. (2012). Clathrin and phosphatidylinositol-4,5-bisphosphate regulate autophagic lysosome reformation. *Nat. Cell Biol.* **14**, 924-934.

Sattler, T. and Mayer, A. (2000). Cell-free reconstitution of microautophagic vacuole invagination and vesicle formation. *J. Cell Biol.* **151**, 529-538.

Schulze, R. J., Weller, S. G., Schroeder, B., Krueger, E. W., Chi, S., Casey, C. A. and McNiven, M. A. (2013). Lipid droplet breakdown requires dynamin 2 for vesiculation of autolysosomal tubules in hepatocytes. *J. Cell Biol.* **203**, 315-326.

Seaman, M. N. J. (2004). Cargo-selective endosomal sorting for retrieval to the Golgi requires retromer. *J. Cell Biol.* **165**, 111-122.

Seaman, M. N. J. (2012). The retromer complex - endosomal protein recycling and beyond. *J. Cell Sci.* **125**, 4693-4702.

Seaman, M. N., Marcusson, E. G., Cereghino, J. L. and Emr, S. D. (1997). Endosome to Golgi retrieval of the vacuolar protein sorting receptor, Vps10p, requires the function of the VPS29, VPS30, and VPS35 gene products. *J. Cell Biol.* **137**, 79-92.

Seaman, M. N., McCaffery, J. M. and Emr, S. D. (1998). A membrane coat complex essential for endosome-to-Golgi retrograde transport in yeast. *J. Cell Biol.* **142**, 665-681.

Seaman, M. N. J., Harbour, M. E., Tattersall, D., Read, E. and Bright, N. (2009). Membrane recruitment of the cargo-selective retromer subcomplex is catalysed by the small GTPase Rab7 and inhibited by the Rab-GAP TBC1D5. *J. Cell Sci.* **122**, 2371-2382.

Smaczynska-de Rooij, I. I., Allwood, E. G., Mishra, R., Booth, W. I., Aghamohammadzadeh, S., Goldberg, M. W. and Ayscough, K. R. (2012). Yeast dynamin Vps1 and amphiphysin Rvs167 function together during endocytosis. *Traffic* **13**, 317-328.

Thorngren, N., Collins, K. M., Fratti, R. A., Wickner, W. and Merz, A. J. (2004). A soluble SNARE drives rapid docking, bypassing ATP and Sec17/18p for vacuole fusion. *EMBO J.* **23**, 2765-2776.

van Weering, J. R. T., Sessions, R. B., Traer, C. J., Kloer, D. P., Bhatia, V. K., Stamou, D., Carlsson, S. R., Hurley, J. H. and Cullen, P. J. (2012a). Molecular basis for SNX-BAR-mediated assembly of distinct endosomal sorting tubules. *EMBO J.* **31**, 4466-4480.

van Weering, J. R. T., Verkade, P. and Cullen, P. J. (2012b). SNX-BAR-mediated endosome tubulation is co-ordinated with endosome maturation. *Traffic* **13**, 94-107.

Vida, T. A. and Emr, S. D. (1995). A new vital stain for visualizing vacuolar membrane dynamics and endocytosis in yeast. *J. Cell Biol.* **128**, 779-792.

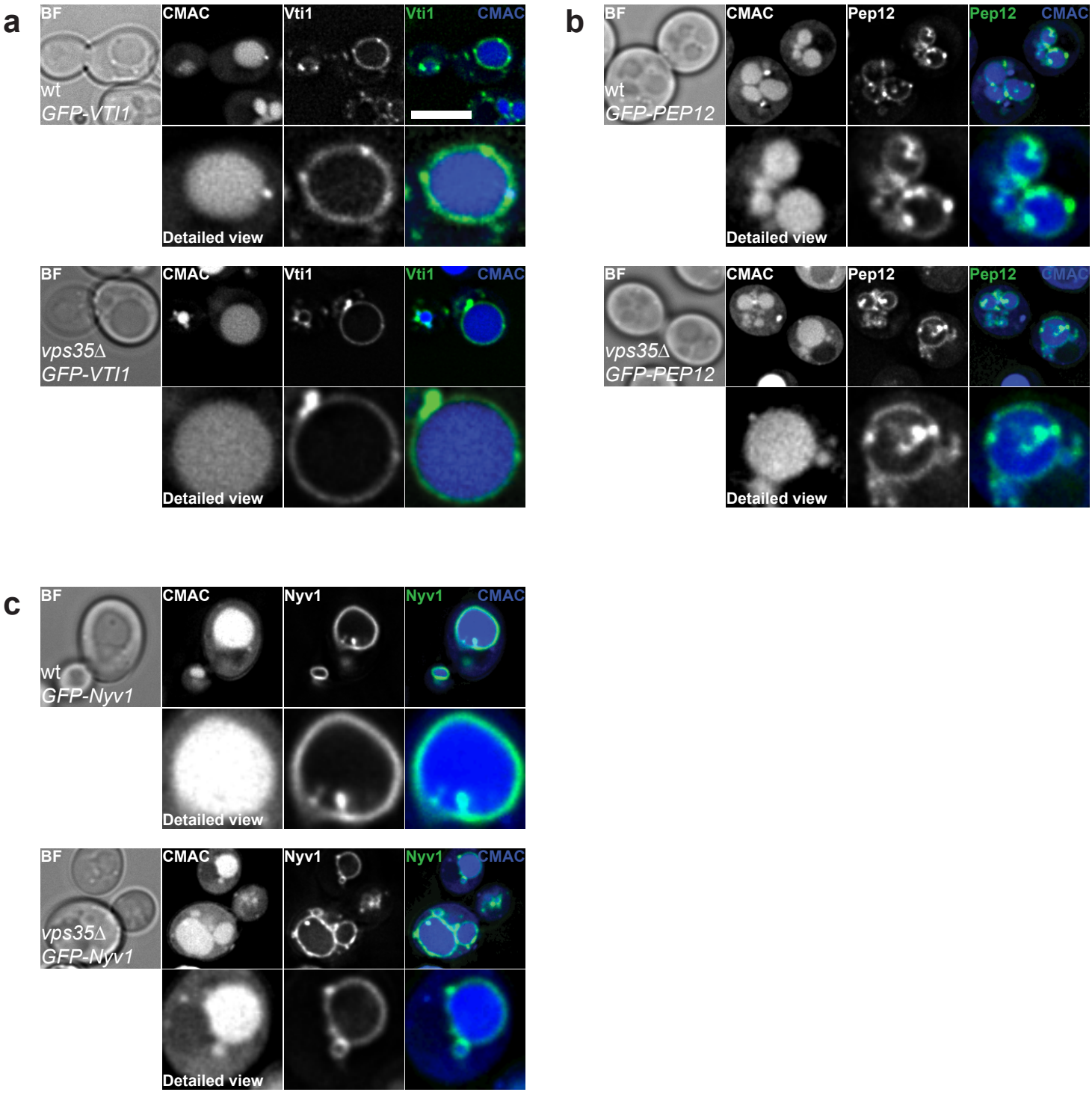

Figure S1. Localization of vacuolar SNAREs in retromer mutants. (a-c) Localization of GFP-tagged SNARE proteins was investigated in wild-type and *vps35*Δ cells. (a) Chromosomal *VTI1* was N-terminally tagged with GFP under control of the intermediate *PHO5* promoter. (b,c) *GFP-PEP12* and *GFP-NYV1* under control of the *TPI1* promoter were expressed from a centromeric plasmids pCU2701 (Pep12) and pCU2702 (Nyv1). Size bar, 5 µm.

Table S1. *Saccharomyces cerevisiae* strains used in this study.

Strain	Genotype	Reference
BY4741	MATa *his3*Δ1 *leu2*Δ0 *met15*Δ0 *ura3*Δ0	EUROSCARF library
BY4727	MATalpha *his3*Δ200 *leu2*Δ0 *lys2*Δ0 *met15*Δ0 *trp1*Δ63 *ura3*Δ0	EUROSCARF library
BJ3505	MATa *pep4*Δ*::HIS3 prb1-*Δ*1.6R lys2-208 trp1*Δ101 *ura3-52 gal2*	Haas *et al.*, 1995
DKY6281	MATalpha *leu2-3 leu2-112 ura3-52 his3-*Δ200 *trp1-*Δ101 *lys2-801 suc2-*Δ*9 PHO8::TRP1*	Haas *et al.*, 1995
SEY6210	MATalpha *leu2-3,122 ura3-52 his3-*Δ*200 trp-*Δ*901 lys2-801 suc2-*Δ *GAL1*	Robinson et al., 1988
CUY4411	BY4727; *VPS17::GFP-kanMX4*	Balderhaar et al., 2010
CUY4412	BY4727; *VPS26::GFP-kanMX4*	Balderhaar et al., 2010
CUY4571	BY4727; *VPS10::GFP-kanMX6*	Balderhaar et al., 2010
CUY4573	BY4741; *vps26*Δ*::kanMX6 VPS10::GFP-HIS3*	Markgraf et al., 2009
CUY6133	BY4727; *VPS35::yeGFP-hphNT1*	This study
CUY6597	BJ3505; *vps35*Δ*::hphNT1*	This study
CUY6599	BJ3505; *vps17*Δ*::hphNT1*	This study
CUY7569	BJ3505; *vps26*Δ*::kanMX6*	This study
CUY7573	BJ3505; *vps17*Δ*::hphNT1 vps5*Δ*::kanMX6*	This study
CUY7575	BJ3505; *vps5*Δ*::kanMX6*	This study
CUY7837	BY4727; *VPS29::GFP-TRP1*	This study
CUY7848	SEY6210; VPS26*::3xmCherry-hphNT1*	This study
CUY9003	BY4741; *VPS10::natNT1-GAL1pr VPS10::GFP-HIS3 vps26*Δ*::kanMX6*	This study
CUY9004	BY4727; *VPS10::natNT1-GAL1pr VPS10::GFP-kanMX6*	This study
CUY9062	BY4727; *VPS10::natNT1-GAL1pr VPS10::GFP-kanMX6 vac8*Δ*::hphNT1*	This study
CUY9063	BY4727; *VPS10::natNT1-GAL1pr VPS10::GFP-kanMX6 vps5*Δ*::hphNT1*	This study
CUY9064	BY4727; *VPS10::natNT1-GAL1pr VPS10::GFP-kanMX6 VPS35::mCherry-TRP1*	This study
CUY9065	BY4727; *VPS10::natNT1-GAL1pr VPS10::GFP-kanMX6 ypt7*Δ*::hphNT1*	This study
CUY9204	BY4727; *VPS10::natNT1-GAL1pr VPS10::GFP-kanMX6 YPT7::URA3-PHO5pr-mCherry*	This study
CUY9209	BY4741; *VMA2::yeGFP-hphNT1*	This study
CUY9212	BY4741; *VMA2::yeGFP-hphNT1 vps35*Δ*::kanMX6*	This study
CUY9213	BY4727; *VPS10::GFP-kanMX6 ypt7*Δ*::hphNT1*	This study
CUY9221	BY4741; *VAM3::URA3-PHO5pr-GFP*	This study
CUY9223	BY4727; *VPS10::natNT1-GALSpr VPS10::GFP-kanMX6*	This study
CUY9330	BY4727; *VPS10::natNT1-GAL1pr VPS10::GFP-kanMX6 VPS1::mCherry-TRP1*	This study
CUY9331	BY4727; *VPS10::natNT1-GAL1pr VPS10::GFP-kanMX6 YPT6::URA3-PHO5pr-mCherry*	This study
CUY9332	BY4727; *VPS10::natNT1-GAL1pr VPS10::GFP-kanMX6 mon1*Δ*::LEU2*	This study
CUY9346	BY4727; *VPS10::natNT1-GAL1pr VPS10::GFP-kanMX6 vps1*Δ*::hphNT1*	This study
CUY9347	BJ3505; *vps1*Δ*::hphNT1*	This study
CUY9348	BY4727; *VPS10::GFP-kanMX6 ypt7*Δ*::hphNT1 vps26*Δ*::TRP1*	This study
CUY9399	BY4727; *VPS10::natNT1-GAL1pr VPS10::GFP-kanMX6 VPS8-3xmCherry-hphNT1*	This study
CUY9400	BY4727; *VPS10::natNT1-GAL1pr VPS10::GFP-kanMX6 apl5*Δ*::hphNT1*	This study
CUY9411	BY4727; *VPS10::natNT1-GAL1pr VPS10::GFP-kanMX6 mvp1*Δ*::TRP1*	This study
CUY9417	BY4727; *VPS26::GFP-kanMX4 vps1*Δ*::natNT1*	This study
CUY9418	BY4727; *VPS35::yeGFP-hphNT1 vps1*Δ*::natNT1*	This study

CUY9498	BY4727; *VPS10::natNT1-GAL1pr VPS10::GFP-kanMX6 vac7Δ::TRP1*	This study
CUY9499	BY4727; *VPS10::natNT1-GAL1pr VPS10::GFP-kanMX6 erv14Δ::TRP1*	This study
CUY9500	BY4727; *VPS10::natNT1-GAL1pr VPS10::GFP-kanMX6 btn2Δ::TRP1*	This study
CUY9501	BY4727; *VPS10::natNT1-GAL1pr VPS10::GFP-kanMX6 btn1Δ::TRP1*	This study
CUY9502	BY4727; *VPS10::natNT1-GAL1pr VPS10::GFP-kanMX6 btn3Δ::TRP1*	This study
CUY9511	BY4727; *VPS10::natNT1-GAL1pr VPS10::GFP-kanMX6 SEC7::mCherry-hphNT1*	This study
CUY9563	BY4727; *VPS10::natNT1-GAL1pr VPS10::GFP-kanMX6 VPS17::mCherry-TRP1*	This study
CUY9569	BY4727; *VPS10::natNT1-GAL1pr VPS10::GFP-kanMX6 vps29Δ::hphNT1*	This study
CUY9570	BY4727; *VPS10::natNT1-GAL1pr VPS10::GFP-kanMX6 vps35Δ::TRP1*	This study
CUY9576	BY4727; *VPS10::natNT1-GAL1pr VPS10::GFP-kanMX6 msb3Δ::TRP1*	This study
CUY9577	BY4727; *VPS10::natNT1-GAL1pr VPS10::GFP-kanMX6 gyp7Δ::TRP1*	This study
CUY9581	BY4727; *VPS10::natNT1-GAL1pr VPS10::GFP-kanMX6 msb4Δ::TRP1*	This study
CUY9623	BY4727; *VPS17::GFP-kanMX4 vps1Δ::TRP1*	This study
CUY9624	BY4741; *VAM3::URA3-PHO5pr-GFP vps1Δ::hphNT1*	This study
CUY9705	BY4727; *VPS10::GFP-kanMX6 mvp1Δ::TRP1*	This study
CUY9708	BY4727; *VPS10ΔC*(1-1490aa)*::GFP-TRP1*	This study
CUY9709	BY4727; *VPS10::natNT1-GAL1pr VPS10ΔC*(1-1490aa)*::GFP-TRP1*	This study